Learning Adaptive Dexterous Grasping from Single Demonstrations

Liangzhi Shi^{1,2*}, Yulin Liu^{1*}, Lingqi Zeng^{1*}, Bo Ai¹, Zhengdong Hong¹, and Hao Su^{1,3}

¹University of California, San Diego

²Tsinghua University

³Hillbot

Abstract—How can robots learn dexterous grasping skills efficiently and apply them adaptively based on user instructions? This work tackles two key challenges: efficient skill acquisition from limited human demonstrations and contextdriven skill selection. We introduce AdaDexGrasp, a framework that learns a library of grasping skills from a single human demonstration per skill and selects the most suitable one using a vision-language model (VLM). To improve sample efficiency, we propose a trajectory following reward that guides reinforcement learning (RL) toward states close to a human demonstration while allowing flexibility in exploration. To learn beyond the single demonstration, we employ curriculum learning, progressively increasing object pose variations to enhance robustness. At deployment, a VLM retrieves the appropriate skill based on user instructions, bridging low-level learned skills with highlevel intent. We evaluate AdaDexGrasp in both simulation and real-world settings, showing that our approach significantly improves RL efficiency and enables learning human-like grasp strategies across varied object configurations. Finally, we demonstrate zero-shot transfer of our learned policies to a realworld PSYONIC Ability Hand, with a 90% success rate across objects, significantly outperforming the baseline.

I. Introduction

Imagine handing a power drill to a teammate during assembly. We naturally grasp it from the top for an easy handoff, but grip the handle when using it ourselves. Humans instinctively adjust their grasp to the task, while robots often rely on fixed strategies. Even learning a single dexterous grasp is challenging due to the hand's high degrees of freedom. How can robots acquire varied grasping skills and apply them adaptively?

The first challenge is to acquire dexterous grasping skills efficiently. Classical robotic control relies on perfect state information, which is often impractical due to perception challenges [1]–[4]. Learning-based approaches attempt to mitigate this by leveraging human demonstrations through imitation learning, which requires extensive data collection and specialized hardware [5]–[8], or reinforcement learning (RL), which suffers from low sample efficiency due to the large state and action space [9], [10]. In this work, we hypothesize that the structural similarity between human and robot hands makes human data a useful *prior*, not perfect demonstrations, for robotic dexterous grasping. While a small number of demonstrations may effectively guide exploration in RL, the optimal way to leverage imperfect demonstrations remains an open question.

Grounding robot actions in context is another challenge. Vision-language action models (VLAs) attempt to map language and images directly to robot actions but require massive datasets and typically focus on kinematically simple

end-effectors, such as parallel grippers [11]–[14]. Inspired by prior work leveraging vision-language models for language-guided task planning [15]–[19], we aim to integrate learned grasping skills with a language-driven selection mechanism to enable adaptive grasping.

To this end, we introduce AdaDexGrasp, a framework with three key components. First, we propose a trajectory following that encourages an RL agent to visit states close to a reference trajectory, which is obtained from a human demonstration via retargeting. This improves sample efficiency while preserving human-like grasping strategies. Second, we introduce a curriculum learning scheme that gradually randomizes the initial object pose, allowing the policy to generalize beyond the single demonstration. Finally, we construct a skill library using the learned policies and query a vision-language model to select the most appropriate skill based on user preferences at deployment.

We extensively evaluate AdaDexGrasp in both simulation and the real world. Our results show that the proposed reward function alone significantly improves sample efficiency, raising the success rate from near zero to an average of 64%. In addition, the proposed curriculum learning strategy further enables the policy to handle varied object configurations not present in human demonstrations. To bridge high-level instructions with low-level execution, our vision-language model achieves a 90% success rate in selecting the appropriate grasping skill based on user input. Finally, we deploy our policy on a real-world PSYONIC Ability Hand, achieving a success rate above 90% consistently, while the baseline struggles to grasp the object successfully.

II. RELATED WORK

A. Dexterous Manipulation

Dexterous manipulation is highly challenging due to the high degree of freedom of the end effector. Traditional methods that use trajectory optimization [2]–[4], [20] require precise modeling of robot dynamics, which is difficult in the open world. In contrast, learning-based methods seek to obtain an observation-to-action mapping from data. Reinforcement learning methods [21]–[24] often require extensive exploration in simulation and specific reward engineering. In addition, the learned grasping policies from reward engineering could be unnatural when compared with human. Imitation learning methods [25], [26] are able to leverage real-world data collected with teleoperation systems [6]–[8], but real-robot data is costly to acquire and the policy is limited by the quality and amount of expert demonstrations. In this work, we aim to leverage a single real-world human demonstration to accelerate reinforcement learning, alleviate

^{*} Equal contribution.

the burden for reward engineering, and acquire human-like grasp poses while using a learning curriculum to enable generalization beyond the demonstrated object configuration.

B. Learning from Human-Object Interaction Data

Human-object interaction datasets with 3D human pose and 6-DoF object pose annotations (e.g., [27]–[29]) provide rich resources for learning dexterous manipulation. [30] extracts robot and object poses from human videos for imitation learning, but suffers from noisy state-action pairs and relies on hundreds of demonstrations and extensive reward tuning. To overcome these issues, [10] proposes a trajectory mapping reward for one-shot learning, using trajectory augmentation and policy distillation to improve generalization. However, this reward is suboptimal as it enforces alignment with potentially flawed demonstrations. Other methods generate humanobject trajectories as RL references [31], or refine imperfect policies learned from retargeted demonstrations via RL or imitation [32]. In contrast, we learn a grasping skill library using a trajectory following reward and curriculum learning, enabling sample-efficient, human-like grasp acquisition and adaptive skill selection.

C. Language-Grounded Manipulation

Aligning robot behaviors with human preference is an important research direction [33], [34]. Language instructions are widely used to convey human preferences [35]–[39], and prior work [11]–[14] has developed Vision-Language-Action (VLA) models to enable robots to follow language commands. However, these models primarily focus on high-level task specifications rather than low-level control variations, such as different grasp poses.

An alternative approach to incorporating human preferences leverages Vision-Language Models (VLMs) [40], [41] with structured skill libraries [17]–[19], [42], [43]. These methods use VLMs to interpret language instructions, extract preference-related information, and retrieve suitable skills from a predefined set. While effective in various manipulation tasks, their application to dexterous manipulation remains limited, particularly in adapting grasp poses to user intent. This work extends the paradigm by building a skill library from human demonstrations and integrating a VLM to enable preference-driven grasp selection, bridging the gap between language understanding and dexterous control.

III. METHOD

A. Overview

The objective of this work is to enable human-like, preference-aware dexterous grasping. To achieve this, the robot must be able to acquire diverse grasping strategies and select the most appropriate one based on human instructions.

We approach this problem by first learning a library of grasping skills from human demonstrations and then developing a mechanism to select a skill based on environment observations and natural language commands. Each skill in the library is trained via reinforcement learning with trajectory guidance, improving the sampling efficiency of learning

while ensuring that the learned grasping behaviors resemble human demonstrations. Given an environment observation, a natural language instruction, and a set of skill descriptions, a selection module determines the best skill for execution.

Formally, we define the problem as a Markov Decision Process (MDP) $\mathcal{M}=(\mathcal{S},\mathcal{A},P,r,\gamma)$. At each time step t, the robot observes the state $s_t\in\mathcal{S}$ and selects an action a_t according to a skill policy π :

$$a_t \sim \pi(a_t \mid s_t).$$

The environment then transitss to a new state s_{t+1} according to the dynamics model P, and the robot receives a reward r_t . Each skill policy $\pi_i \in \Pi$ is optimized to maximize the expected cumulative reward given a reference trajectory extracted from a human demonstration τ_i :

$$\pi^* = \arg\max_{\pi} \mathbb{E}\left[\sum_{t=0}^{H} \gamma^t r(s_t, a_t, s_{t+1} \mid \tau_i)\right],$$

where H is the task horizon. The reference τ_i (e.g., a human grasping video) both guides learning for sample efficiency and promotes human-like behavior.

Once the skill library is learned, we introduce a skill selection function Ψ . Given an environment image P, a natural language instruction I, and a set of skills with language descriptions Π , Ψ retrieves the most suitable skill for execution:

$$\pi^* = \Psi(P, I, \Pi).$$

This framework allows the robot to acquire grasping strategies from single human demonstrations and adapt its grasp based on preferences in human instruction. Next, we detail how we extract human demonstrations (Section III-B), train policies with trajectory guidance (Section III-C) via curriculum learning (Section III-D), and how the selection module enables preference-aware grasping (Section III-E).

B. Human Videos as Robot Demonstrations

To obtain human demonstrations, we use the DexYCB dataset, which provides real-world video recordings along with ground-truth hand and object poses for various objects [27]. Each object has demonstrations with at least two initial positions and two grasp poses. We seek to translate human demonstrations to robot trajectories to guide downstream reinforcement learning.

The challenge lies in overcoming the embodiment gap between human data and robot hardware. To this end, we first translate human hand motions into robot joint positions to ensure kinematic feasibility with the robotic system. Since the extracted hand poses from DexYCB are floating and not attached to an arm, we explicitly anchor the robot hand to an arm to maintain realistic motion representation. The translation process consists of two steps: (i) retargeting hand motion, where human hand motions are mapped to the robot's hand joint positions, and (ii) solving joint positions of the arm with inverse kinematics (IK). This process enables the robot to replicate human grasping strategies while maintaining kinematic constraints.

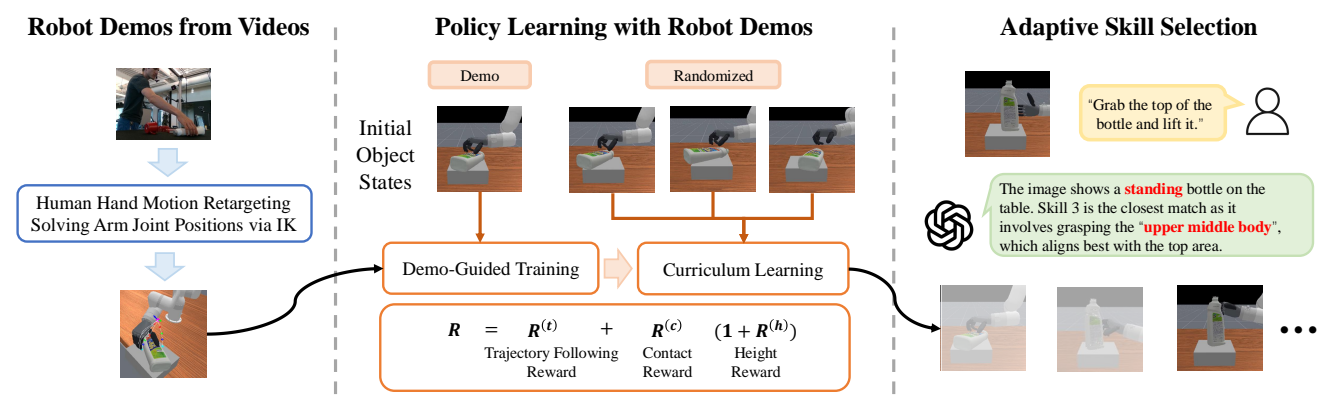


Fig. 1: Method overview. AdaDexGrasp consists of three key components: (i) Converting human videos into robot demonstrations via motion retargeting, (ii) learning a grasp policy through trajectory-guided reinforcement learning with a curriculum, and (iii) skill selection using vision-language models to ground robot behavior into user preference.

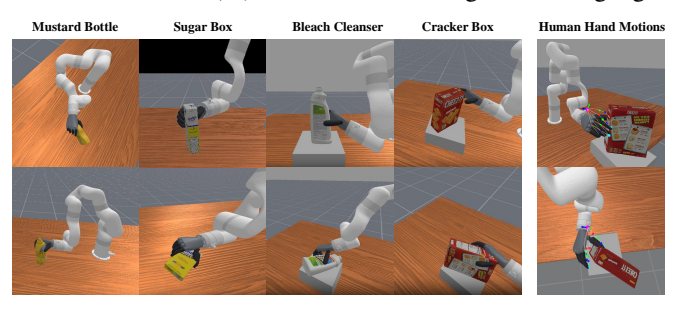


Fig. 2: Example robot demonstrations converted from human videos in the DexYCB dataset. The Ability Hand with xArm7 replicates human grasps under different object poses.

Hand motion retargeting. Following [6], [7], [10], [44], [45], we adopt an optimization-based approach. The goal is to minimize the difference between the fingertip positions of the robot hand and those of the human hand. The loss function is:

$$\mathcal{L}_{\text{retarget}}(q_k) = \sum_{i=1}^{5} \|x_k^i - f_i(q_k)\|^2 + \beta \|q_k - q_{k-1}\|^2,$$

subject to:

$$q_l \le q_k \le q_u$$

where q_k denotes the robot hand joint positions at time k, x_k^i is the i-th fingertip position of the human hand, $f_i(q_k)$ represents the corresponding i-th fingertip of robot hand given q_k via forward kinematics, and q_l and q_u are the lower and upper bound limits of the joint positions. An additional penalty term weighted by β enhances temporal smoothness. We perform optimization using the NLopt solver [6].

Computing arm joints via IK. Given end-effector poses from the retargeted robot hand trajectory, we compute the joint positions of the arm using Closed-Loop Inverse Kinematics (CLIK) with the Pinocchio library [46], [47].

Since human hand motion follows a minimum jerk trajectory [48], which reduces joint errors [49] and minimizes mechanical wear [50], we apply post-processing to the joint position sequence $\{q_k\}_{k=0}^{T-1}$ using the model from [51], following [30]. Fig. 2 illustrates examples of motion retargeting with an Ability hand mounted on an xArm7.

C. Reward Function Designs

Our goal is to leverage human demonstrations to learn natural, human-like grasping strategies at high sample efficiency. We achieve this with a trajectory following reward that encourages the policy to stay close to the reference trajectory. Since human demonstrations may not perfectly translate to robotic execution due to differences in morphology and kinematics, the robot must balance guidance with exploration. To address this, we design a reward scheme that integrates the trajectory following reward with other rewards that measure task progression.

Trajectory following reward. The reward guides the robot hand toward the pre-grasp stage. Existing work [10] enforces state-to-state alignment between the robot trajectory and the reference trajectory, which can be overly restrictive, as human demonstrations may contain suboptimal or infeasible motions. Instead, agents should flexibly reach key states using their own strategies while leveraging demonstrations. To achieve this, we propose a reward that measures the proximity of robot states and the reference trajectory, inspired by TR^2 [52]. The reward at time step t is defined as:

$$R_t^{(t)} = \begin{cases} r_{\text{dist}}(s_t, d_{k_{\text{max}}(s_t)}) \cdot (\eta + \beta \cdot k_{\text{max}}(s_t)), \\ \text{if } k_{\text{max}}(s_t) > \max_{0 \le t' < t} k_{\text{max}}(s_{t'}), \\ 0, \quad \text{otherwise.} \end{cases}$$

where $k_{\max}(s_t) = \max_{0 \leq k < T} \{k \mid \operatorname{dist}(s_t, d_k) < \epsilon\}$, tracks the furthest state in the reference trajectory that the policy has matched so far. Here, T is the length of the reference trajectory, which may differ from the episode length H. The function $\operatorname{dist}(s,d)$ measures the distance between state s and a reference state s, defined as:

$$\operatorname{dist}(s,d) = \sum_{i=1}^5 \alpha_1 \|s^{i,\operatorname{pos}} - d^{i,\operatorname{pos}}\|_2 + \alpha_2 \operatorname{rad}(s^{i,\operatorname{rot}},d^{i,\operatorname{rot}}).$$

Here, state $s^{i,*}, d^{i,*}$ denotes the relative pose of the i-th fingertip to the object, with pos, rot indicating position and rotation, respectively. $r_{\rm dist}(s,d)$ is defined as: $r_{\rm dist}(s,d) = 1 - \tanh({\rm dist}(s,d))$, mapping the distance to a bounded reward that encourages the policy to reach states closer to

the reference. In this paper, we refer to our reward and that in [10] as the trajectory following and trajectory mapping reward, respectively.

We empirically set $\alpha_1=1,\alpha_2=0.03,\eta=30,\beta=0.2,$ and $\epsilon=0.04$. The reward is assigned only when the policy makes progress toward reaching a further state in the reference trajectory. Once the robot hand reaches the object, the reward value remains zero as the furthest matched state index jumps to the last frame. As a result, the reward only guides the policy up to the pre-grasp stage.

Contact reward. A stable grasp requires sufficient contact between the hand and the object. Inspired by the concept of force closure in grasp generation [53], [54], a grasp is considered force-closure if there exist contact forces $\{f_i\}$ at contact points $\{x_i\}$ within the friction cones rooted at x_i that can resist arbitrary external wrenches. While force-closure provides a robust measure of grasp stability, directly enforcing it is computationally complex. Instead, we design a heuristic contact reward $(R^{(c)})$ that is assigned when the thumb and at least two other fingers make contact with the object. This encourages grasps that approximate force-closure without requiring explicit force analysis.

Height reward. To ensure task completion, we introduce a height reward $(R^{(h)})$, which is proportional to the object's height and provides an additional bonus when the object reaches the target height. This encourages the policy to complete the grasping task rather than stopping prematurely.

The final reward at time t is defined as:

$$R_t = R_t^{(t)} + R_t^{(c)} (1 + R_t^{(h)}).$$

D. Curriculum Learning

While the reward terms guide the learner to follow the reference and discover feasible robot trajectories, the policy may struggle to generalize to diverse initial object poses due to variation in demonstrations. To improve generalization, we use curriculum learning, gradually increasing task difficulty to expose the policy to a wider range of object configurations.

Initially, we use one fixed object's pose for learning so that the policy quickly discovers feasible grasp poses. We then gradually randomize the initial pose, defined as a tuple of position and rotation $(p^{\text{pos}}, p^{\text{rot}})$: $p^{\text{pos}} \sim \mathcal{U}(p^{\text{pos}}_{\text{init}} - \sigma P_{\text{max}}, p^{\text{pos}}_{\text{init}} + \sigma P_{\text{max}})$, $p^{\text{rot}} \sim \mathcal{U}(p^{\text{rot}}_{\text{init}} - \sigma \Theta_{\text{max}}, p^{\text{rot}}_{\text{init}} + \sigma \Theta_{\text{max}})$ where $(p^{\text{pos}}_{\text{init}}, p^{\text{rot}}_{\text{init}})$ is the original pose, \mathcal{U} stands for uniform distribution, P_{max} and Θ_{max} represent the maximum position displace in x,y and the maximum rotation deviation around the z-axis, respectively. The noise factor $\sigma \in [0,1]$ controls the degree of variation, which is initialized as 0 and increased incrementally by 0.01 until reaching 1 after the performance exceeds a predefined success threshold ζ . This ensures that the policy learns to generalize to diverse object configurations at a high sample efficiency.

E. Adaptive Skill Selection

Curriculum learning allows us to train a diverse set of grasping policies, $\Pi = \{\pi_i\}_{i=0}^{N-1}$, each corresponding to a different grasp pose. However, selecting the most appropriate policy based on human preference remains a challenge. To

address this, we introduce a Vision-Language Model (VLM)-based agent as a decision-making module that retrieves the optimal skill from the skill library Π . Given a human instruction I in natural language, the VLM processes the instruction, environment image, and skill descriptions to infer the most suitable grasping policy. The selected policy is then executed, ensuring alignment with human intent and the environmental context.

IV. EXPERIMENTS

In this section, we investigate the following questions:

- Does our framework enable sample-efficient acquisition of generalizable human-like grasp strategies?
- Is our vision-language model-based skill selection adaptable to varying user preferences?
- Can the policy learned in simulation transfer effectively to the real world?

A. Evaluating the Learning Framwork

1) Evaluation Setup: Task setup. We focus on four objects from DexYCB [27] dataset: mustard-bottle, bleach-cleanser, cracker-box, and sugar-box. For each object, we select two videos, each featuring a different initial position and grasp pose. To evaluate our learning framework for skill library construction, we train a separate policy for each object-pose combination. Performance is measured by the success rate (SR), defined as the proportion of successful object lifts that reach a sufficient height. Each experiment is repeated five times with independent trials, and we report the average performance metrics.

Simulation environment. We use a PSYONIC Ability Hand on an xArm 7, matching our real-world hardware setup. Training and testing are conducted in ManiSkill3 [55], a SAPIEN-powered [56] framework that enables realistic environments and fast GPU-parallelized training.

Implementation. We adopt Proximal Policy Optimization (PPO) [57] for policy learning. The robot observes the full simulation state, including all joint angles, and the poses of the hand, fingertips, and objects, represented in the robot arm base frame. The policy outputs joint angle deltas, indicating real-time changes for actuation. For each object and grasp pose, we train the policy for 80M steps with a fixed initial pose, followed by another 120M steps using the proposed curriculum. During curriculum training, we randomize object position within ± 5 cm in xy and rotation within $\pm 30^\circ$ around the z-axis. A success is defined as lifting the object above 20 cm. At test time, we evaluate the policy on varied initial object configurations, using the same randomization as in curriculum training.

2) Main Results: We compare our method with the state-of-the-art ViViDex [10], which uses a trajectory mapping reward to aid RL training, followed by imitation learning on rollouts for better generalization. The observation and action spaces are the same as in AdaDexGrasp. For fair comparison, we trained both our reimplementation of ViViDex and AdaDexGrasp for 200M steps. Our proposed reward design differs in several aspects. In the pre-grasp stage,

SR (%) ↑	mustaro	d-bottle pose-2	bleach- pose-1	-cleanser pose-2	cracke pose-1	er-box pose-2	suga:	r-box pose-2	Avg
ViViDex [10]	0.00	0.02	0.00	0.00	0.00	0.39	0.04	0.00	0.06
ViViDex (w/ curriculum) Ours	0.00 61.45	$0.00 \\ 84.38$	0.00 98.89	0.00 99.55	0.00 76.56	11.74 94 . 24	0.08 67.34	0.00 98.61	1.48 85 . 12

TABLE I: Quantitative results in simulation. We evaluate our policies, each trained to learn different grasp poses from distinct human demonstrations, on objects with varying visual appearances, sizes, and physical properties.

we reward object approach and contact. These are retained during manipulation, with an added reward for object motion alignment. To address sim-demo length mismatch, we use progress-based frame selection. The object-approach reward extends ViViDex with rotation-aware distance, while the contact reward follows Section III-C. To ensure fairness, we use the same randomized initial object poses from our curriculum training for both training and testing. In addition, we implement a version of ViViDex with our proposed learning curriculum, which differs from AdaDexGrasp only in the reward function design, for a more controlled comparison.

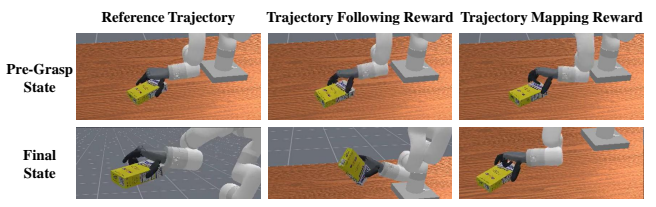
Our results show that ViViDex struggles with our demonstration dataset, even with our proposed curriculum. This is likely due to its sensitivity to the morphological gap between the human hand and the robot. The Ability Hand's smaller size requires greater precision in grasping, while the trajectory mapping reward enforces strict alignment with the imperfect reference trajectory extracted from human demonstration. This highlights the robustness of our reward function, which we further analyze in Section IV-A.3.

3) Analysis of Trajectory Following vs. Trajectory Mapping Reward: To compare trajectory following and trajectory mapping rewards, we implement a variant using trajectory mapping reward and conduct experiments on sugar-box pose-2. We measure the sum of fingertip distances from the demonstration's pre-grasp frame and track object height.

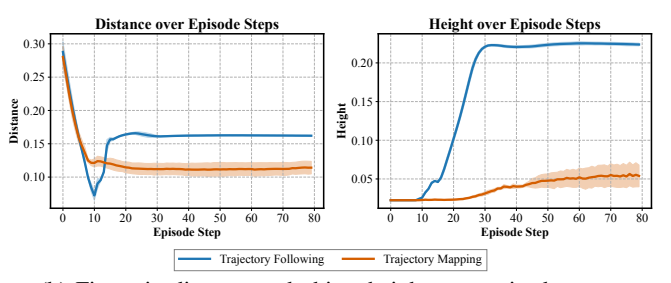
As shown in Figure 3, our reward function enables the robot to achieve a grasp pose closer to the demonstration before contact. However, after grasping, the fingertip distance increases, exceeding that of trajectory mapping. The success of our policy, despite this deviation, suggests that strict adherence to the reference trajectory is not always optimal. Human demonstrations are inherently imperfect for robots due to morphological differences, and motion retargeting introduces additional approximation errors. Unlike trajectory mapping, our reward function allows flexibility in execution, enabling the RL policy to refine the grasp for better effectiveness.

4) Ablation Study of Reward Terms: We conduct ablation studies across eight grasping environments with fixed initial object poses. We compare our full pipeline with variations where each reward term is omitted. Without contact rewards, height rewards are given without contact checks. Without height rewards, we remove the height-proportional reward but retain the success reward when the object reaches the target height. The results are shown in Fig. II.

The baseline without trajectory following reward shows near-zero success, failing in eight environments, indicating its crucial role in reducing the sample space for RL training. While the variant without contact reward performs well in three environments, it struggles in others, showing its impor-



(a) Illustration of pre-grasp and final grasp states.



(b) Fingertip distance and object height over episode steps.

Fig. 3: Comparison between the proposed trajectory following reward and a standard trajectory mapping reward.

tance in refining hand-object interactions despite imperfect demonstrations. Similarly, removing the height reward lowers success rates, highlighting its role in guiding the policy with goal-related information.

5) Effects of Curriculum Learning: To evaluate the impact of curriculum learning on training efficiency, we conduct experiments on sugar-box tasks with two grasp poses. We first train a policy for 80M steps using a fixed initial object pose. Training then continues for an additional 120M steps, during which we systematically vary the success threshold ζ to analyze its effect. Additionally, we compare with direct training, where the policy is trained from the beginning with the same level of object pose randomization as at the end of curriculum learning.

During the early stages of curriculum learning, the task success rate initially declines before stabilizing around the success threshold ζ . As the success rate remains near ζ , the noise level gradually increases. Once the noise level reaches its final value, $\sigma=1$, the task success rate surpasses ζ .

We observe that a lower success threshold causes a faster rise in noise level. However, when comparing the steps at which different settings reach the same success rate after the noise level hits 1, a higher threshold yields greater training efficiency. This suggests that maintaining a high success rate while gradually introducing noise during curriculum learning offers better sample efficiency than rapidly increasing noise. Furthermore, direct training results in a significantly lower success rate, underscoring the effectiveness of curriculum learning in improving RL training efficiency.

SR (%) ↑	mustaro	d-bottle pose-2	bleach- pose-1	-cleanser pose-2	cracke pose-1	er-box pose-2	suga:	r-box pose-2	Avg
w/o trajectory following w/o contact reward	0.00 59.80	0.00	0.00	19.94 0.00	0.00 40.00	0.02 83.98	0.00 79.69	$0.00 \\ 39.94$	2.50 37.93
w/o height reward	79.94	79.92	27.50	0.00	60.00	77.29	39.80	20.00	48.06
Ours	79.84	39.84	39.90	39.92	79.94	96.48	79.63	59.34	64.36

TABLE II: Ablation study in simulation. We evaluate the impact of removing individual design components and demonstrate that our full pipeline achieves the best performance.

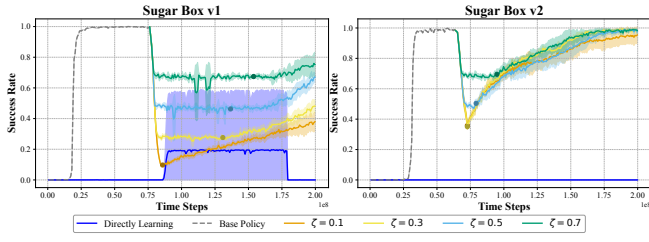


Fig. 4: Comparison of sample efficiency between direct learning from fully random initial object pose and curriculum learning with different success thresholds (ζ). The circular dot represents the average timestep at which σ reaches 1. A suitable ζ leads to faster convergence and better performance.

P(skill task) (%)	T1	T2	Т3	T4	T5
Skill 1 Skill 2	28 72	100	0 100	0	0
Skill 3	0	0	0	100	100

TABLE III: The percentage of times each skill is selected for a given task. The Vision-Language Model (VLM) consistently assigns specific skills to tasks, indicating structured decision-making rather than random selection.

B. Evaluating Adaptive Skill Selection

1) Evaluation Setup: Task setup. We evaluate the performance of the VLM-based agent for adaptive skill selection through a series of tasks designed to account for both the object's initial positions and human preference. Experiments are conducted on bleach-cleanser following the settings in Section IV-A. The VLM operates based on two key principles: (i) ensuring successful object grasping and (ii) taking into account human preferences.

Using our proposed RL training framework, we obtain three distinct skills (S1-S3): (i) Skill 1: Grasp the *bottom* of a standing bottle and lift it. (ii) Skill 2: Grasp the *upper middle* of a standing bottle and lift it. (iii) Skill 3: Grasp a lying bottle, rotate it upright, and lift it.

We define five tasks that vary based on the object's initial pose and the given human preference: (i) T1: Standing, no preference. (ii) T2: Standing, grasp *bottom*. (iii) T3: Standing, grasp *top*. (iv) T4: Lying, no preference. (v) T5: Lying, grasp *bottom* (conflicting instruction). In T3, the term *top* is intentionally ambiguous, as it differs from the *upper middle* grasp described in S2. In T5, the instruction contradicts the object's initial pose, evaluating the VLM's ability to resolve conflicting grasping instructions.

Implementation. We use GPT-4 as the VLM. Given an environment image, human instructions, and descriptions of each skill, the VLM outputs the number of the selected skill along with a rationale for the choice in no more than

SR (%) ↑	T1	T2	Т3	T4	T5
Random Selection	44	64	64	24	52
VLM-based Selection	96	76	100	96	96

TABLE IV: Overall success rates of skill selection and execution. The table compares a random selection policy with a VLM-based policy, showing that VLM improves both skill selection and execution success.

three sentences. Once the VLM selects a skill, the robot executes the corresponding policy to complete the task. Each task is evaluated 25 times with varying initial object poses. To assess the effectiveness of our method, we introduce a random selection baseline. This baseline randomly selects a skill from the skill library and executes it without considering the environment image or human instructions.

2) **Results**: Skill selection results are reported in Table III. In T1, the VLM selects either S1 or S3. However, when a clear human preference is given (T2 and T3), the VLM reliably chooses the skill that best aligns with the request. In T4 and T5, the VLM prefers S3, as S1 and S2 are designed for a standing bottle. Even when instructed to grasp the bottom of a lying bottle (T5), the VLM selects S3 to ensure a feasible grasp. This shows that the VLM is able to consider both human intent and environmental context.

In terms of overall task success rate (Table IV), random selection often fails to choose the appropriate skill. In contrast, VLM-based selection aligns with human preferences and achieves high task success.

C. Real World Experiments

1) Evaluation Setup: Task setup. We validate the sim-to-real transfer of our policies on a real robot. We focus on three objects with varying geometry, appearance, and mass distributions: mustard-bottle, bleach-cleanser, and cracker-box. For each object, we use the first grasp pose and apply a random $\pm 20^{\circ}$ rotation and a ± 3 cm position shift, repeating the experiment ten times.

Hardware setup. We use a PSYONIC Ability Hand mounted on an xArm 7 for real-world experiments. A RealSense D435i depth camera is calibrated using [58] to capture RGB-D data for object pose estimation.

Implementation. We use FoundationPose [59] as our object pose estimator, which estimates object pose given object meshes, RGB-D observations, and object segmentation masks. At the start of each experiment, we provide a bounding box of the target object in the input image and use Segment Anything (SAM) [60] to extract its mask. After estimating the object pose, we initialize the object's position in simulation to match the real-world setup and execute



(a) Grasping and lifting a bleach cleanser bottle.

(b) Grasping and lifting a cracker box.

Fig. 5: Qualitative results illustrating the grasping process for the mustard-bottle and cracker-box. The images show the robot approaching, grasping, and lifting each object with two different grasp poses.

SR (%) ↑	mustard-bottle	bleach-cleanser	cracker-box
ViViDex [10]	0	0	0
Ours	90	100	90

TABLE V: Real-world manipulation results on objects with varying geometry, visual appearance, and physical properties. Our method outperforms the baseline by a large margin.

the policy for one episode of 80 time steps. The resulting robot joint positions serve as tracking targets for the real robot. This approach reduces the sim-to-real gap compared to directly executing policy outputs, ensuring the real-world behavior aligns more closely with simulation [61].

2) **Results**: As shown in Table V, our method consistently achieves strong performance, maintaining at least a 90% success rate across objects. In contrast, the baseline fails on all three objects, as expected given its near-zero success rate in simulation. Figure 5 shows qualitative results, illustrating the robot grasping objects with different poses.

V. CONCLUSION & LIMITATIONS

We introduced AdaDexGrasp, a framework for efficiently learning and adaptively selecting dexterous grasping skills. By integrating human demonstrations, demonstration-guided reinforcement learning, curriculum learning, and VLM-based skill selection, AdaDexGrasp enables sample-efficient acquisition of diverse, human-like grasps. We demonstrate strong performance in both simulation and real-world experiments.

Our approach has a few limitations. First, as the skill library scales to include more grasp and object types, retrieving the appropriate policy becomes more susceptible to hallucinations by VLMs. Structured knowledge representations (e.g., symbolic) may help encode skill affordances [43] and support more reliable information update and reasoning [62]. Second, while we test the model on simple, ambiguous instructions, its robustness to more complex or noisy language inputs remains to be explored. These challenges open promising directions for future work.

REFERENCES

- [1] K. He, R. Newbury, T. Tran, J. Haviland, B. Burgess-Limerick, D. Kulić, P. Corke, and A. Cosgun, "Visibility maximization controller for robotic manipulation," *IEEE Robotics and Automation Letters*, vol. 7, no. 3, pp. 8479–8486, 2022.
- [2] D. Rus, "In-hand dexterous manipulation of piecewise-smooth 3-d objects," *The International Journal of Robotics Research*, vol. 18, no. 4, pp. 355–381, 1999.

- [3] I. Mordatch, Z. Popović, and E. Todorov, "Contact-invariant optimization for hand manipulation," in *Proceedings of the ACM SIG-GRAPH/Eurographics symposium on computer animation*, pp. 137–144, 2012.
- [4] A. Wu, M. Guo, and C. K. Liu, "Learning diverse and physically feasible dexterous grasps with generative model and bilevel optimization," arXiv preprint arXiv:2207.00195, 2022.
- [5] A. Brohan, N. Brown, J. Carbajal, Y. Chebotar, J. Dabis, C. Finn, K. Gopalakrishnan, K. Hausman, A. Herzog, J. Hsu, et al., "Rt-1: Robotics transformer for real-world control at scale," arXiv preprint arXiv:2212.06817, 2022.
- [6] Y. Qin, W. Yang, B. Huang, K. Van Wyk, H. Su, X. Wang, Y.-W. Chao, and D. Fox, "Anyteleop: A general vision-based dexterous robot arm-hand teleoperation system," arXiv preprint arXiv:2307.04577, 2023.
- [7] R. Ding, Y. Qin, J. Zhu, C. Jia, S. Yang, R. Yang, X. Qi, and X. Wang, "Bunny-visionpro: Real-time bimanual dexterous teleoperation for imitation learning," arXiv preprint arXiv:2407.03162, 2024.
- [8] C. Wang, H. Shi, W. Wang, R. Zhang, L. Fei-Fei, and C. K. Liu, "Dexcap: Scalable and portable mocap data collection system for dexterous manipulation," arXiv preprint arXiv:2403.07788, 2024.
- [9] A. Rajeswaran, V. Kumar, A. Gupta, G. Vezzani, J. Schulman, E. Todorov, and S. Levine, "Learning complex dexterous manipulation with deep reinforcement learning and demonstrations," arXiv preprint arXiv:1709.10087, 2017.
- [10] Z. Chen, S. Chen, E. Arlaud, I. Laptev, and C. Schmid, "Vividex: Learning vision-based dexterous manipulation from human videos," arXiv preprint arXiv:2404.15709, 2024.
- [11] M. Kim et al., "Openvla: An open-source vision-language-action model," arXiv preprint arXiv:2406.09246, 2024.
- [12] Octo Model Team, D. Ghosh, H. Walke, K. Pertsch, K. Black, O. Mees, S. Dasari, J. Hejna, and e. Charles Xu, "Octo: An opensource generalist robot policy," in *Proceedings of Robotics: Science* and Systems, (Delft, Netherlands), 2024.
- [13] A. Brohan, N. Brown, J. Carbajal, Y. Chebotar, X. Chen, K. Choromanski, and e. Tianli Ding, "Rt-2: Vision-language-action models transfer web knowledge to robotic control," in arXiv preprint arXiv:2307.15818, 2023.
- [14] S. Liu, L. Wu, B. Li, H. Tan, H. Chen, Z. Wang, K. Xu, H. Su, and J. Zhu, "Rdt-1b: a diffusion foundation model for bimanual manipulation," arXiv preprint arXiv:2410.07864, 2024.
- [15] Z. Yang, C. Garrett, D. Fox, T. Lozano-Pérez, and L. P. Kaelbling, "Guiding long-horizon task and motion planning with vision language models," arXiv preprint arXiv:2410.02193, 2024.
- [16] K. Shirai, C. C. Beltran-Hernandez, M. Hamaya, A. Hashimoto, S. Tanaka, K. Kawaharazuka, K. Tanaka, Y. Ushiku, and S. Mori, "Vision-language interpreter for robot task planning," in 2024 IEEE International Conference on Robotics and Automation (ICRA), pp. 2051–2058, 2024.
- [17] Z. Wu, B. Ai, and D. Hsu, "Integrating common sense and planning with large language models for room tidying," in RSS 2023 Workshop on Learning for Task and Motion Planning, 2023.
- [18] M. Ahn et al., "Do as i can and not as i say: Grounding language in robotic affordances," arXiv preprint, vol. arXiv:2204.01691, 2022.
- [19] J. Liang, W. Huang, F. Xia, P. Xu, K. Hausman, B. Ichter, P. Florence, and A. Zeng, "Code as policies: Language model programs for embodied control," in arXiv preprint arXiv:2209.07753, 2022.
- [20] Z. He, B. Ai, Y. Liu, W. Wan, H. I. Christensen, and H. Su, "Learning dexterous deformable object manipulation through cross-embodiment dynamics learning," in 3rd RSS Workshop on Dexterous Manipulation: Learning and Control with Diverse Data, 2025.

- [21] H. Qi, B. Yi, S. Suresh, M. Lambeta, Y. Ma, R. Calandra, and J. Malik, "General in-hand object rotation with vision and touch," in *Conference on Robot Learning*, pp. 2549–2564, PMLR, 2023.
- [22] Y. Yuan, H. Che, Y. Qin, B. Huang, Z.-H. Yin, K.-W. Lee, Y. Wu, S.-C. Lim, and X. Wang, "Robot synesthesia: In-hand manipulation with visuotactile sensing," in 2024 IEEE International Conference on Robotics and Automation (ICRA), pp. 6558–6565, IEEE, 2024.
- [23] J. Wang, Y. Yuan, H. Che, H. Qi, Y. Ma, J. Malik, and X. Wang, "Lessons from learning to spin" pens"," arXiv preprint arXiv:2407.18902, 2024.
- [24] Z. Hong, Y. Liu, H. Hou, B. Ai, J. Wang, T. Mu, Y. Qin, J. Gu, and H. Su, "Learning particle-based world model from human for robot dexterous manipulation," in 3rd RSS Workshop on Dexterous Manipulation: Learning and Control with Diverse Data, 2025.
- [25] M. Bain and C. Sammut, "A framework for behavioural cloning.," in Machine intelligence 15, pp. 103–129, 1995.
- [26] C. Chi, Z. Xu, S. Feng, E. Cousineau, Y. Du, B. Burchfiel, R. Tedrake, and S. Song, "Diffusion policy: Visuomotor policy learning via action diffusion," *The International Journal of Robotics Research*, p. 02783649241273668, 2023.
- [27] Y.-W. Chao, W. Yang, Y. Xiang, P. Molchanov, A. Handa, J. Tremblay, Y. S. Narang, K. Van Wyk, U. Iqbal, S. Birchfield, et al., "Dexycb: A benchmark for capturing hand grasping of objects," in *Proceedings of* the IEEE/CVF conference on computer vision and pattern recognition, pp. 9044–9053, 2021.
- [28] Z. Fan, O. Taheri, D. Tzionas, M. Kocabas, M. Kaufmann, M. J. Black, and O. Hilliges, "Arctic: A dataset for dexterous bimanual hand-object manipulation," in *Proceedings of the IEEE/CVF Conference on Computer Vision and Pattern Recognition*, pp. 12943–12954, 2023.
- [29] Y. Liu, Y. Liu, and e. Jiang, Che, "Hoi4d: A 4d egocentric dataset for category-level human-object interaction," in *Proceedings of the IEEE/CVF Conference on Computer Vision and Pattern Recognition*, pp. 21013–21022, 2022.
- [30] Y. Qin, Y.-H. Wu, and e. Liu, Shaowei, "Dexmy: Imitation learning for dexterous manipulation from human videos," in *European Conference* on *Computer Vision*, pp. 570–587, Springer, 2022.
- [31] Y. Chen, C. Wang, Y. Yang, and C. K. Liu, "Object-centric dexterous manipulation from human motion data," arXiv preprint arXiv:2411.04005, 2024.
- [32] H. G. Singh, A. Loquercio, C. Sferrazza, J. Wu, H. Qi, P. Abbeel, and J. Malik, "Hand-object interaction pretraining from videos," arXiv preprint arXiv:2409.08273, 2024.
- [33] Y. Wang, L. Wang, Y. Du, B. Sundaralingam, X. Yang, Y.-W. Chao, C. Perez-D'Arpino, D. Fox, and J. Shah, "Inference-time policy steering through human interactions," arXiv:2411.16627, 2024.
- [34] S. Belkhale, T. Ding, T. Xiao, P. Sermanet, Q. Vuong, J. Tompson, Y. Chebotar, D. Dwibedi, and D. Sadigh, "Rt-h: Action hierarchies using language," in https://arxiv.org/abs/2403.01823, 2024.
- [35] J. Luketina, N. Nardelli, G. Farquhar, J. Foerster, J. Andreas, E. Grefenstette, S. Whiteson, and T. Rocktäschel, "A survey of reinforcement learning informed by natural language," arXiv preprint arXiv:1906.03926, 2019.
- [36] E. Jang, A. Irpan, M. Khansari, and e. Kappler, Daniel, "Bc-z: Zero-shot task generalization with robotic imitation learning," in *Conference on Robot Learning*, pp. 991–1002, PMLR, 2022.
- [37] S. Stepputtis, J. Campbell, M. Phielipp, S. Lee, C. Baral, and H. Ben Amor, "Language-conditioned imitation learning for robot manipulation tasks," *Advances in Neural Information Processing Systems*, vol. 33, pp. 13139–13150, 2020.
- [38] M. Shridhar, L. Manuelli, and D. Fox, "Cliport: What and where pathways for robotic manipulation," in *Conference on robot learning*, pp. 894–906, PMLR, 2022.
- [39] O. Mees, L. Hermann, and W. Burgard, "What matters in language conditioned robotic imitation learning over unstructured data," *IEEE R-AL*, vol. 7, no. 4, pp. 11205–11212, 2022.
- [40] Q. Gao, X. Pi, K. Liu, J. Chen, R. Yang, X. Huang, X. Fang, L. Sun, G. Kishore, B. Ai, et al., "Do vision-language models have internal world models? towards an atomic evaluation," arXiv preprint arXiv:2506.21876, 2025.
- [41] R. Bommasani, D. A. Hudson, E. Adeli, R. Altman, S. Arora, S. von Arx, M. S. Bernstein, J. Bohg, A. Bosselut, E. Brunskill, et al., "On the opportunities and risks of foundation models," arXiv preprint arXiv:2108.07258, 2021.
- [42] L. Zha, Y. Cui, L.-H. Lin, M. Kwon, M. G. Arenas, A. Zeng, F. Xia,

- and D. Sadigh, "Distilling and retrieving generalizable knowledge for robot manipulation via language corrections," 2023.
- [43] Z. Wu, B. Ai, T. Silver, and T. Bhattacharjee, "Savor: Skill affordance learning from visuo-haptic perception for robot-assisted bite acquisition," arXiv preprint arXiv:2506.02353, 2025.
- [44] A. Handa and e. Van Wyk, Karl, "Dexpilot: Vision-based teleoperation of dexterous robotic hand-arm system," in 2020 IEEE International Conference on Robotics and Automation (ICRA), pp. 9164–9170, IEEE, 2020.
- [45] D. Antotsiou, G. Garcia-Hernando, and T.-K. Kim, "Task-oriented hand motion retargeting for dexterous manipulation imitation," in Proceedings of the European conference on computer vision (ECCV) workshops, pp. 0–0, 2018.
- [46] J. Carpentier, F. Valenza, N. Mansard, et al., "Pinocchio: fast forward and inverse dynamics for poly-articulated systems." https://stack-oftasks.github.io/pinocchio, 2015–2021.
- [47] J. Carpentier, G. Saurel, G. Buondonno, J. Mirabel, F. Lamiraux, O. Stasse, and N. Mansard, "The pinocchio c++ library – a fast and flexible implementation of rigid body dynamics algorithms and their analytical derivatives," in *IEEE International Symposium on System Integrations (SII)*, 2019.
- [48] T. Flash and N. Hogan, "The coordination of arm movements: an experimentally confirmed mathematical model," *Journal of neuroscience*, vol. 5, no. 7, pp. 1688–1703, 1985.
- [49] K. J. Kyriakopoulos and G. N. Saridis, "Minimum jerk path generation," in *Proceedings*. 1988 IEEE international conference on robotics and automation, pp. 364–369, IEEE, 1988.
- [50] F. Merat, "Introduction to robotics: Mechanics and control," *IEEE Journal on Robotics and Automation*, vol. 3, no. 2, pp. 166–166, 1987.
- [51] E. Todorov and M. I. Jordan, "Smoothness maximization along a predefined path accurately predicts the speed profiles of complex arm movements," *Journal of Neurophysiology*, pp. 696–714, 1998.
- [52] S. Tao, X. Li, T. Mu, Z. Huang, Y. Qin, and H. Su, "Abstract-to-executable trajectory translation for one-shot task generalization," in *International Conference on Machine Learning, ICML 2023, 23-29 July 2023, Honolulu, Hawaii, USA* (A. Krause, E. Brunskill, K. Cho, B. Engelhardt, S. Sabato, and J. Scarlett, eds.), vol. 202 of *Proceedings of Machine Learning Research*, pp. 33850–33882, PMLR, 2023.
- [53] T. Liu, Z. Liu, Z. Jiao, Y. Zhu, and S.-C. Zhu, "Synthesizing diverse and physically stable grasps with arbitrary hand structures using differentiable force closure estimator," *IEEE Robotics and Automation Letters*, vol. 7, no. 1, pp. 470–477, 2021.
- [54] R. Wang, J. Zhang, J. Chen, Y. Xu, P. Li, T. Liu, and H. Wang, "Dexgraspnet: A large-scale robotic dexterous grasp dataset for general objects based on simulation," in 2023 IEEE International Conference on Robotics and Automation (ICRA), pp. 11359–11366, IEEE, 2023.
- [55] S. Tao, F. Xiang, A. Shukla, Y. Qin, X. Hinrichsen, X. Yuan, C. Bao, X. Lin, Y. Liu, T.-k. Chan, et al., "Maniskill3: Gpu parallelized robotics simulation and rendering for generalizable embodied ai," arXiv preprint arXiv:2410.00425, 2024.
- [56] F. Xiang, Y. Qin, K. Mo, Y. Xia, H. Zhu, F. Liu, M. Liu, H. Jiang, Y. Yuan, H. Wang, et al., "Sapien: A simulated part-based interactive environment," in *Proceedings of the IEEE/CVF conference on computer vision and pattern recognition*, pp. 11097–11107, 2020.
- [57] J. Schulman, F. Wolski, P. Dhariwal, A. Radford, and O. Klimov, "Proximal policy optimization algorithms," arXiv preprint arXiv:1707.06347, 2017.
- [58] Z. Hong, K. Zheng, and L. Chen, "Fully automatic hand-eye calibration with pretrained image models," *International Conference on Intelligent Robots and Systems (IROS)*, 2024.
- [59] B. Wen, W. Yang, J. Kautz, and S. Birchfield, "Foundationpose: Unified 6d pose estimation and tracking of novel objects," in CVPR, pp. 17868–17879, 2024.
- [60] A. Kirillov, E. Mintun, N. Ravi, H. Mao, C. Rolland, L. Gustafson, T. Xiao, S. Whitehead, A. C. Berg, W.-Y. Lo, et al., "Segment anything," in CVPR, pp. 4015–4026, 2023.
- [61] X. Liu, J. Adalibieke, Q. Han, Y. Qin, and L. Yi, "Dextrack: Towards generalizable neural tracking control for dexterous manipulation from human references," arXiv preprint arXiv:2502.09614, 2025.
- [62] R. Chen, W. Jiang, C. Qin, I. S. Rawal, C. Tan, D. Choi, B. Xiong, and B. Ai, "LLM-based multi-hop question answering with knowledge graph integration in evolving environments," in *Findings of the Association for Computational Linguistics: EMNLP 2024* (Y. Al-Onaizan, M. Bansal, and Y.-N. Chen, eds.), (Miami, Florida, USA), pp. 14438–14451, Association for Computational Linguistics, Nov. 2024.